Fire-Balls in Pion Multiple Production

——Brasil-Japan Collaboration of Chacaltaya Emulsion Chamber Experiment——

Jose A. CHINELLATO, Carola DOBRIGKEIT, J. Bellandi FILHO, Cesar M. G. LATTES, Marcio J. MENON, Carlos E. NAVIA O., Ammiraju PEMMARAJU, Kotaro SAWAYANAGI, Edison H. SHIBUYA and Armando TURTELLI Jr.

Instituto de Fisica Gleb Wataghin, Universidade Estadual de Campinas Campinas, S. P.

Neuza M. AMATO, Naoyuki ARATA and F. M. Oliveira CASTRO

Centro Brasileiro de Pesquisas Fisicas, Rio de Janeiro, R. J.

Regina H. C. MALDONADO

Instituto de Fisica, Universidade Federal Fluminense, Niteroi, R. J.

Hiroshi AOKI, Yoichi FUJIMOTO, Shunichi HASEGAWA, Hiroshi SEMBA, Masanobu TAMADA, Kojiro TANAKA and Seibun YAMASHITA

Science and Engineering Research Laboratory, Waseda University Tokyo 162

Toru SHIBATA and Kei YOKOI

Department of Physics, Aoyama Gakuin University, Tokyo 157

Hiroshi KUMANO, Akinori OHSAWA and Takaaki TABUKI

Institute for Cosmic Ray Research, University of Tokyo Tanashi, Tokyo 188

(Received August 26, 1982; Revised February 14, 1983)

The article describes a study of the multiple pion production through observation of gamma-rays produced by nuclear interactions at the target layer of the emulsion chambers exposed at Chacaltaya, Bolivia, 5200 m above sea level. The analysis was focused on 80 events with $\Sigma E_\gamma > 20$ TeV, well above the detection threshold of the X-ray film spot scanning, ~3 TeV. The distribution of gamma-rays is constructed on their energy, p_t, and emission angle, and the comparison is made with the results from the simulation calculations based on FNAL hydrogen bubble chamber events and ISR minimum bias events. The cosmic-ray results are significantly out of the simple

scaling extrapolation, showing higher rapidity density n_γ and increasing p_t. Recent $\bar{p}$-p collider experiments gave the confirming results.

From the plot of events in the diagram of n_γ and $\langle p_t \rangle$, the events are classified into two types; Mirim-jets (meaning small jets, $n_\gamma = 2 \sim 3$, $\langle p_t \rangle \sim 140$ MeV/c) and Açu-jets (large jets, $n_\gamma = 6 \sim 8$, $\langle p_t \rangle \sim 220$ MeV/c), with nearly equal frequency of production. Mirim-jets are those on the scaling extrapolation from the lower energy region of accelerators, while increasing rate of Açu-jets with energy is causing the scaling break. The analysis with the fire-ball model shows that the Mirim-jets are consistently interpreted as production and decay of a small fire-ball (a fire-ball quantum called H-quantum) with rest energy of 2~3 GeV and decay temperature of about 130 MeV. While, the Açu-jets necessitate introduction of a heavy fire-ball (SH-quantum) with rest energy of 20~30 GeV.

The study of atmospheric interactions (A-jets) shows presence of events with still larger n_γ and higher p_t, which are called Guaçu-jets. One C-jet is found to be a candidate of this type. The Guaçu-jets require presence of a huge fire-ball (UH-quantum) of rest energy 200~300 GeV.

Discussions are made on physical implication of the fire-ball model, particularly on those quanta of a fire-ball.

§ 1. Fire-ball model

1.1. *Historical background*

The idea of a fire-ball came up long time ago, around the period when the phenomena of hadron multiple production were started to be observed by cosmic-ray experiments. One can find pioneer work of Wataghin in 1941,[1] in which he introduced an idea of a fire-ball from his cosmic-ray experiment on penetrating showers (meson showers in the present terminology). Wataghin, as a theoretician, was one of those who proposed the cutoff method to remove the ultra-violet divergences in the field theory. He was not satisfied with the cutoff procedure as being just a mathematical trick to avoid the divergences, but he thought that it must be connected to some yet unknown physical object of real existence. Thus he imagined creation of an isotropic fire-ball at rest in the center of a nuclear collision, which has a fixed temperature, $kT \sim 3m_\pi c^2$, equal to the meson energy with the cutoff momentum. According to him, the cutoff procedure is a mathematical expression of the newly introduced substance, i.e., the fire-ball. The model naturally predicts the multiplicity law proportional to the square-root of the incident energy, $N \sim E_0^{1/2}$.

The most familiar one among earlier attempts of the fire-ball model will be the one proposed by Fermi in 1950.[2] He visualized the nuclear collision as an interaction between the two approaching meson clouds, which have a thin disc form because of the Lorentz contraction due to their motion. At the moment of a collision, the strong interaction between mesons makes the whole amount of their kinetic energy be liberated into a small region of overlapping discs. The created object, thin disc-shaped dense gas of mutually interacting mesons,

dose not immediately fly away into pieces, but undergoes complicated meson-meson interactions in itself. After attaining a sort of thermal equilibrium among the constituent mesons, the object turns into a cluster of freely outgoing mesons. Thus he anticipated that the emitted mesons will be with statistical distribution of energy similar to the one of black-body radiation. From such argument, he derived the multiplicity law proportional to a power of one quarter of the incident energy, $N \sim E_0^{1/4}$.

Most of early models of fire-ball were with analogy to the classical physics and were easy to be understood. People thought that large multiplicity in meson production would allow such classical analogy because of high quantum number of the participating states. Thus, in the days of 1950's, a number of cosmic-ray experiments were made in analysis of their data with reference to the fire-ball models. We will describe here essence of the achievements which played important roles for the later development.

Let us start with the experimental study on temperature of a fire-ball, which was made by the following two methods. One is to measure the composition of produced hadrons, particularly the abundance of neutral pions among them. Generally, the identification of particle kinds is not easy even now, and was almost impossible in the experiments of those days. The only exception is a neutral pion, which can be identified by its characteristic decay into two gamma-rays. The experiments were made with observation on electron pairs from the decay gamma-rays and also on charged hadrons produced in cosmic-ray jets, supplemented by observation of neutral secondary jets which gives information on neutral hadrons of long life. The experimental data from the primary particle energy range, $10^{11} \sim 10^{12}$ eV, showed that pions are the major component, about 80% of the whole produced hadrons, and heavier particles, such as K-mesons, nucleons and anti-nucleons, and so on, are few. If one applies a thermodynamical argument, the abundances are determined by the magnitude of temperature of a decaying fire-ball, kT, and the rest energy of particles of the concerned kinds. The result shows that the temperature kT is of the order of pion rest energy, $m_\pi c^2$.

The other is to measure the transverse momentum p_t of produced particles. For estimation of p_t, one has to know the particle energy, but it was almost impossible to be measured in the conventional nuclear emulsion stack observation. An accurate energy measurement became feasible only after introduction of the emulsion chamber techniques. The emulsion chamber, a multi-layered sandwich of lead plates and photo-sensitive layers, converts gamma-rays into electron showers and the size measurement of the electron showers can be made with help of the photo-sensitive layers. The shower size gives an energy estimation of the gamma-rays, and then, of the gamma-decaying neutral pions. The result of emulsion chamber experiment showed that p_t-distribution can be approximately expressed in an exponential form, as

the thermodynamical argument had anticipated. The average value, $\langle p_t \rangle$, for neutral pions is found of the order of a few hundred MeV, giving estimation of the temperature kT to be of the order of pion rest energy.

The two ways of estimation on the fire-ball temperature are giving a consistent result, and the observed value,

$$kT \sim m_\pi c^2 , \tag{1}$$

is much smaller than the magnitude of participating energies in the collision, such as the incident energy $E_0{}^*$ in the c.m. system of the collision. This result can be interpreted as expressing a characteristic time in the sequence of processes of multiple production of mesons. For example, the collision itself has a characteristic time,

$$\tau_{\text{collision}} \sim (\hbar/m_\pi c^2)\,(m_N c^2/E_0{}^*), \tag{2}$$

i.e., the time for an incoming nucleon to pass through the Lorentz-contracted meson cloud of the target nucleon, m_N being nucleon rest mass. It is much shorter than the time scale characterizing emission of secondary hadrons, which will be given by the temperature as,

$$\tau_{\text{emission}} \sim \hbar/kT \sim \hbar/m_\pi c^2 . \tag{3}$$

Large difference between the two time constants, $\tau_{\text{collision}}$ in (2) and τ_{emission} in (3), makes plausible our basic assumption that the process of multiple hadron production goes through the two steps, one characterized by $\tau_{\text{collision}}$ for creation of a fire-ball and the other by τ_{emission} for its decay with emission of many hadrons.

Another piece of information was on absorption and attenuation of high energy hadrons of cosmic-rays. The cross section for high energy nuclear interaction was nearly equal to the geometrical cross section of a nucleus, indicating that the cross section for the elementary nucleon-nucleon collision will be not far from the geometrical size of a meson cloud, i.e.,

$$\sigma_{\text{N-N}} \sim \sigma_{\text{geo}} = \pi(\hbar/m_\pi c)^2 . \tag{4}$$

Comparing this with the attenuation of cosmic-ray hadrons through the matter, it was concluded that an incoming hadron with energy E_0 does not dissipate completely in the nuclear collision, but a substantial part of the incident energy is carried out by one of the produced particles——calling it a surviving particle.*) It can be interpreted as being a result of the fact that the nuclear collision is partially inelastic with inelasticity K, and the incoming hadron does not lose its identity and goes out with energy $(1-K)E_0$. The inelasticity K varies from case to case, while its average value $\langle K \rangle$ is found near 0.5.

*) A leading particle in accelerator physics language.

Seeing from the side of a fire-ball, we find from this partial inelasticity that the surviving particle flies away much faster than the fire-ball——a group of produced hadrons——so that the fire-ball must be an independent existence from the outgoing surviving particles.

1.2. *Two fire-ball model*

Particles emitted isotropically from a fire-ball show a characteristic angular distribution which can be approximated by Gaussian function with a fixed width in terms of logtanθ-scale. θ is the emission angle measured from the axis of fire-ball motion in the laboratory system. With the use of the pseudo-rapidity variable, $\xi = -\ln \tan(\theta/2)$, the distribution of hadrons from an isotropic fire-ball is expressed as,

$$f_{\text{F-B}}(\xi)\,d\xi = \frac{n}{(2\pi\sigma)^{1/2}} \exp\left\{-\frac{(\xi-\xi_0)^2}{2\sigma}\right\} d\xi \tag{5}$$

with $\sigma = 1/2$. n expresses number of emitted hadrons and ξ_0 is pseudo-rapidity of the fire-ball, connected to Lorentz factor of its motion as,

$$\xi_0 = \ln 2\Gamma\,. \tag{6}$$

Thus, if the produced fire-ball is isotropic in its hadron emission, it will be easily recognized through the characteristic distribution in logtanθ-plot of observed cosmic-ray jets.

In this period of 1950's, observation of cosmic-ray jets was made mainly with nuclear emulsion stacks, which can give only the geometrical configuration of particle tracks in jets. Thus, the study of angular distribution was the main concern and analysis with logtanθ-plot was considered the most powerful method. The angular distributions observed in those experiments were, in most of the cases, not in agreement with the expected one (5) from an isolated isotropic fire-ball. The distribution in the pseudo-rapidity ξ-scale is much wider, in almost all cases, than the one of isotropic emission. Thus people had to discard the possibility of a single isotropic fire-ball being created at the center of a collision.

The two fire-ball model was proposed under such situation, in 1958, by Niu, also by Kracow group of Miesowitz and others, and by Cocconi, independently.[3] According to the model, the two colliding hadrons emit a respective isotropic fire-ball, as is schematically illustrated in Fig. 1. In this model, the process contains two free parameters, the inelasticity K and rest energy of the created fire-ball, Mc^2. Even for the case of a fixed energy being given to the fire-ball production, the collision system has a freedom to produce either a fast-moving fire-ball with small rest energy, or a slow-moving heavy one. Therefore, the model is able to describe wide varieties of logtanθ-plot seen in

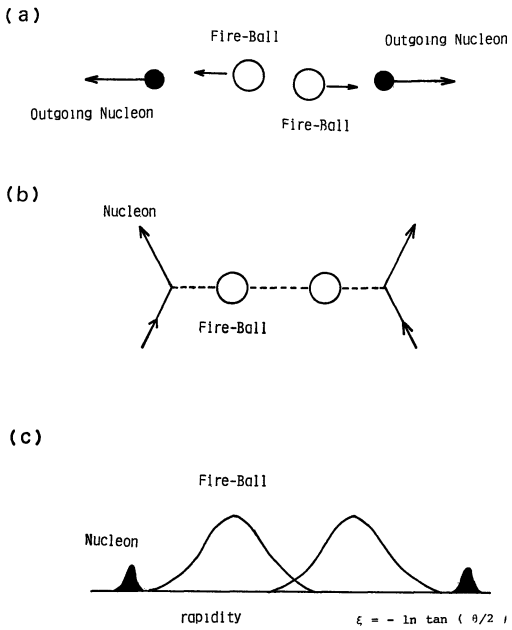

Fig. 1. Two fire-ball model.
(a) Illustration.
(b) Diagram.
(c) logtanθ-plot.

the experiments. If the produced fire-balls overlap each other, the event will be seen just as a single heavy fire-ball case. With partial overlapping between the two, we will observe the object which looks like an elongated ellipsoid, that is, a fire-cigar but not a ball. Only with large relative motion between the two, we will find two bumps in the logtanθ-plot exhibiting existence of the two fire-balls.

The basis of two fire-ball model is partial persistency of the colliding particles. It means that the incoming particles do not totally lose their identity through the collision, but they keep going on with emission of the respective fire-balls. Thus one may guess that the direction of an outgoing surviving particle as well as of its created fire-ball will be along the incident direction. The experimental data on p_t show that it is in fact the case. From such point of view, the collision process can be reduced to a simple one-body problem, where an incoming hadron splits into an out-going hadron and a fire-ball by a shock of the collision. Then, the effect of collision for the fire-ball creation can be reduced to just one parameter, i.e., the magnitude of four-momentum transferred, Δ, during the collision. Then the kinematics gives the following expression for the quantity Δ as,

$$\Delta \sim Mc/2\Gamma^* , \tag{7}$$

where M expresses the fire-ball rest mass and Γ^* Lorentz factor of its motion in the c.m. system. This is obtained under the approximation of neglecting effects from the motion in transversal direction.

It was not easy to prove or disprove clearly the existence of two fire-balls in the collision, while most of the observed jets could be explained by the two fire-balls with suitably chosen parameter values, rest energy, Mc^2, and Lorentz factor, Γ. With such application, Niu was able to make estimation of the four-momentum transfer Δ for every observed cosmic-ray jets, and he obtained the result that Δ is 1–2 GeV/c. We may express the result symbolically, just as we did for the fire-ball temperature kT, as

$$\Delta \sim m_N c \,. \tag{8}$$

The constancy of four-momentum transfer Δ, being always of the order of $m_N c$, gives an interesting consequence. Applying the result (8) to the kinematical relation (7), we have,

$$Mc = (E_0 m_N K^2 \Delta^2)^{1/4} \tag{9}$$

which predicts that the fire-ball rest energy increases proportionally to a power of 1/4 of the incident energy E_0. Under the assumption of constant temperature kT, we arrive at 1/4 power increase in the multiplicity rule, familiar among the cosmic-ray workers.

1.3. *H-quantum model*

The H-quantum model was proposed in 1961 by Hasegawa,[4] in which he assumed existence of an elementary unit of meson multiple production, calling it H-quantum (abbreviation of a heavy quantum). His theoretical motivation was from the composite theory of hadrons, particularly success of Sakata's model. A fire-ball was considered, until then, an object of classical continuum, leaving its rest energy and its temperature as free parameters. He thought that, if hadrons would be not an elementary particle but a composite system, such sub-hadronic structure should appear in the properties of a fire-ball itself. One possibility of this choice was to assume the existence of an elementary unit of a fire-ball, like an atom for the matter or a light quantum for the radiation. In this way, he chose the name, H-quantum, meaning a heavy quantum, for the hypothetical energy quantum of a fire-ball.

The other motivation came from increase of experimental information of cosmic-ray jets of higher energy. It became clear that a substantial part of observed high energy jets, say with $E_0 > 10^{12}$ eV, were hard to be reconciled with the two fire-ball model. Their log$\tan\theta$-plot was, in general, too widely spread to be consistent with the two fire-ball case. The particle distribution is like a wide flat plateau with several maxima and minima. If we try to describe the case with a fire-ball, it was necessary to assume creation of, not just two, but many fire-balls located in a sequence along the direction of collision axis.

In the H-quantum model, the number of produced fire-balls is not restricted

to two, but the size of each fire-ball will be fixed because of being an elementary energy quantum. At moderate energies, the collision will be the creation of two H-quanta, where no difference will be seen between the H-quantum and the two fire-ball case. The difference will appear in higher energy cases, where we will start to observe emission of four, six or more H-quanta, instead of having just two fire-balls in all cases. Those created plural H-quanta will be in a sequence along the line of collision axis. If the relative motion between the neighbouring H-quanta is large enough, we will observe a sequence of isolated hadron clusters in the logtanθ-plot. Otherwise, neighbouring hadron clusters will overlap each other and we will recognize a smooth plateau. Such situation is illustrated in Fig. 2.

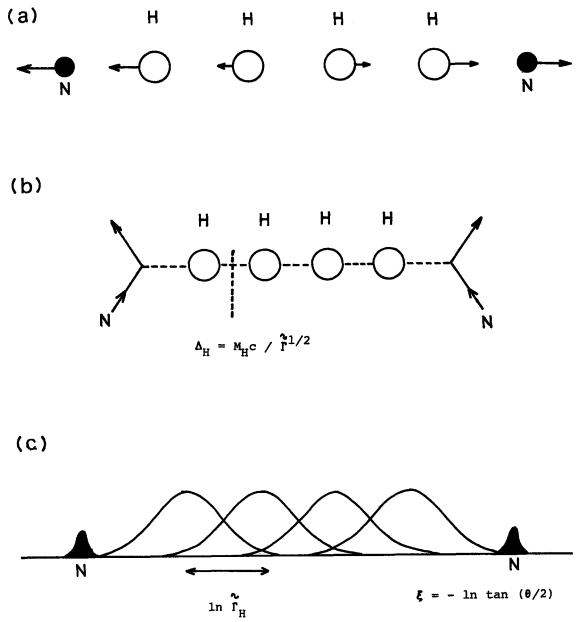

Fig. 2. H-quantum model.
(a) Illustration.
(b) Diagram.
(c) logtanθ-plot.

Hasegawa made analysis of data of jets, and found that the model can describe almost all of logtanθ-plots, and gave the best guess for the free parameters in the model, i.e., the rest energy of H-quantum and its motion in the c.m. system of collision. He estimated average multiplicity from a single H-quantum as $\langle n \rangle \sim 6$, which gives, together with the known value of temperature kT, a guess for the H-quantum rest energy as,

$$M_H c^2 \sim 2 m_N c^2 . \tag{10}$$

The value (10) was what he anticipated from an analogical reasoning with the Sakata model. In the original Sakata model, the constituents of any hadrons are p, n, Λ and the anti-particles, and a pion is assumed to be made by a pair of nucleon and anti-nucleon. Thus he considered that the pion emission

in nucleon anti-nucleon annihilation would represent an elementary act, and the rest energy of H-quantum was expected to be about that of a nucleon pair, $2m_Nc^2$.

On the motion of H-quantum, he noticed a rule that the Lorentz factor of H-quantum in the c.m. system of the collision appears to take only a series of certain discrete values, as $\Gamma_H^* = 1.5, 8.0, 45, \cdots$. He called this regularity "velocity quantization", and tried to connect it with some sub-hadronic mechanism. Later, it was seen that the series of discrete values for Γ_H^* is geometric, so that the rule can be expressed as the relative motion between the neighbouring ones is of constant velocity. Lorentz factor of the relative motion $\tilde{\Gamma}_H$ is found as $\tilde{\Gamma}_H \sim 6$, for all adjacent H-quantum pairs. Assuming the diagram of its creation as in Fig. 2, we are able to estimate the magnitude of four-momentum transferred at every successive creation of an H-quantum. Expressing the quantity as Δ_H, we have a kinematical relation as,

$$\Delta_H = M_H c/\tilde{\Gamma}_H^{1/2}. \tag{11}$$

Putting the above value of $\tilde{\Gamma}_H$, we have $\Delta \sim m_N c$, which is identical to the previous result of (8).

1.4. *Composite particle picture of hadrons*

So far we were concerned with the studies in the period till early 1960's. The H-quantum model was able to give an overall consistent interpretation to the existing data, though the experimental evidence for the existence was not yet conclusive. The situation made us realize importance of improving experimental apparatus for cosmic-ray jets, because the observation by nuclear emulsion stacks on the angular distribution was found not enough for the purpose. That was the time of start of Brasil-Japan collaboration experiment at Mt. Chacaltaya, Bolivia, where we intended to perform a large-scale exposure of emulsion chambers. Details of such direction will be presented in the following sections.

In spite of ambiguities in the experimental conclusions, we were able to draw a perspective of the fire-ball model from estimation of the four-momentum transferred in the collision. The estimation, $\Delta \sim m_N c$ of (8), was obtained both under assumption of the two fire-ball model as well as of H-quantum model. It suggests to us that the estimation of $\Delta \sim m_N c$ will be a general conclusion independent of an assumed type of fire-ball models.

Hasegawa and Yokoi made an attempt to such generalization,[5] with the use of the correspondence between the diagram and the logtanθ-plot of a jet, as is seen in Fig. 3. They divide the whole meson-producing system into two at an angle θ, calling them the forward and backward part, and compute the four-momentum transferred $\Delta(\theta)$ between the two with the following formula,

$$\Delta(\theta)^2 = \langle p_t \rangle^2 \left(\sum_{\text{for}} \tan\theta_i\right)\left(\sum_{\text{back}} \cot\theta_j\right), \tag{12}$$

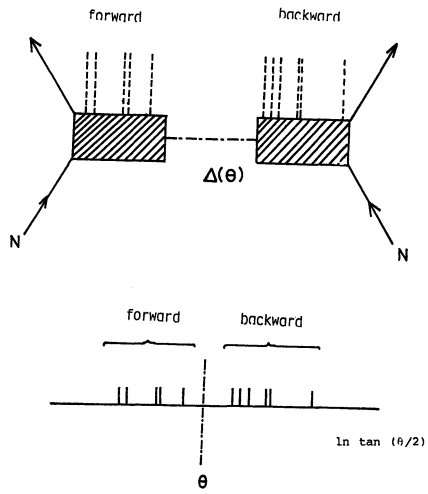

Fig. 3. Estimation of four-momentum transferred $\Delta(\theta)$.

where the summations, $\sum_{\text{for}}$ and $\sum_{\text{back}}$, run over all the produced particles in the forward and the backward part, respectively. They are able to obtain a set of values $\Delta(\theta)$ with varying angle θ, corresponding to a gap between the particles in the logtanθ-plot and choose the minimum value Δ_{min} for a guess to true Δ for the fire-ball creation. It is seen that Δ_{min} thus defined will be identical to Δ, when the fire-balls are isolated and no overlapping exists between the hadron clusters from the neighbouring fire-balls. In case of overlapping, it will give an underestimation, not over. The result obtained by the application to ICEF data[6] tells that the magnitude of Δ is about $m_{\text{N}}c$ or more, but not less.

Thus we were able to obtain two physical constants with dimension of energy, which characterize the multiple meson production. One is the four-momentum transferred Δ with magnitude of nucleon rest energy $m_{\text{N}}c$, characterizing the process of creation of a fire-ball. The other is the temperature kT for the decay of a fire-ball into a hadron cluster and it has magnitude of pion rest energy $m_{\text{N}}c^2$. The estimation is independent from which particular type of fire-ball models we choose to assume.

Now, the cross section of cosmic-ray nuclear interaction is near the geometrical cross section of a nucleus, and, from this, the elementary nucleon collision is considered to have a cross section of the order of area of the surrounding pion cloud, (4). In such cases, we should expect that a large part of the observed events are a distant collision, with the collision parameter b being of the order of pion Compton wave length $\hbar/m_{\pi}c$. The so-called central collison, with the impact parameter b of the order of nucleon Compton wave length $\hbar/m_{\text{N}}c$ or less, would happen only with small probability. Thus, the nuclear collisions, which we are observing most of the cases, will be caused by exchange of a single pion in a cloud, and magnitude of the four-

momentum transferred Δ will be $\sim m_\pi c$. It contradicts with our experimental observation that the majority of cosmic-ray multi-pion production events are with $\Delta \sim m_N c$.

A solution to get out of the apparent contradiction can be found in the view that a pion is not an elementary particle but a composite system. When the energy of incoming particles is high and the width of Lorentz-contracted meson clouds is becoming as thin as $\hbar/m_N c$ or less, then a pion in the colliding clouds will not behave as an elementary particle. Then, the elementary process in the collision of the clouds will be the interaction with exchange of a quantum of the subhadronic medium. Thus the magnitude of the four-momentum transferred during the collision will not be $m_\pi c$ but some increased value characteristic to the subhadronic matter, which we found as $\Delta \sim m_N c$.

In early days of the original Sakata model, the above characteristic value Δ of the subhadronic matter was identified to $m_N c$ without much doubt, because nucleons were considered the constituents for a pion. With the prevailing QCD picture, however, the situation becomes not so straightforward as the above. But, we may conjecture, on the basis of the uncertainty principle, that Δ characterizes size of the subhadronic composite system for a pion. Thus, the composite picture of a hadron will lead us to visualize formation of a tube of hadronic matter connecting the two outgoing meson clouds, i.e., the surviving nucleons. This intermediate product with the width of $\hbar/\Delta$ will split into a series of H-quanta, with partial overlapping. Then, each H-quantum, originally of the size $\sim\hbar/\Delta$ will expand and reach to the size $\sim\hbar/m_\pi c$, where they are ready to transmute into a cluster of pions. Figure 4 demonstrates such view of a collision.

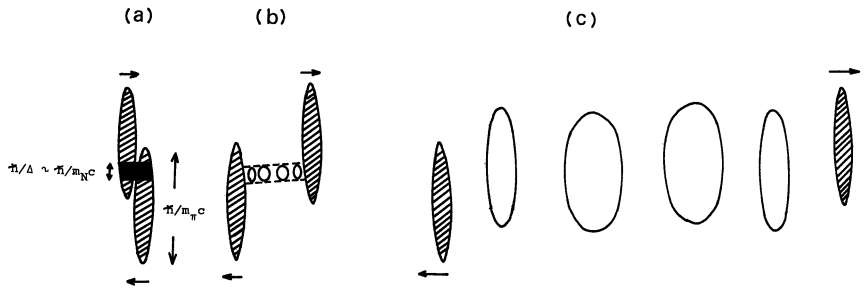

Fig. 4. Distant nuclear collision visualized under the composite particle model.
(a) Localized interaction with dimension $\hbar/\Delta$.
(b) Tube of hadronic matter turns into a series of H-quanta.
(c) H-quanta expand and go to decay into pions.

§ 2. Chacaltaya emulsion chamber experiment

The basic structure of the emulsion chamber is a multi-layered sandwich

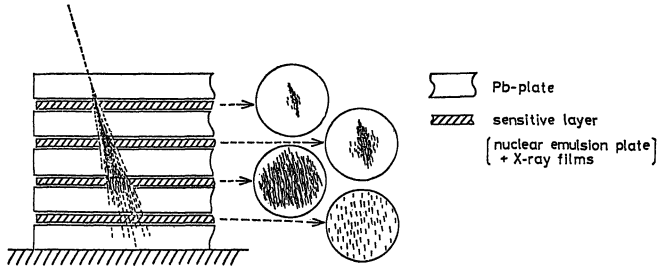

Fig. 5. Emulsion chamber as detector of electron showers.

of lead plates and photo-sensitive layers, as is illustrated in Fig. 5. A gamma-ray or an electron, either coming incident on the chamber from outside or being generated inside the chamber itself, makes an electron shower through the cascade multiplication processes. The generated electron shower is recorded by the photo-sensitive layers composed of highly sensitive X-ray films and a nuclear emulsion plate.

The X-ray film records a shower as a black spot, which is easily recognized by naked eyes, for cases with shower energy greater than 1$\sim$2 TeV. These X-ray films serve for the scanning of shower spots over a large area of the chamber. After knowing location of the shower through the spot in X-ray films, we are able to observe under a microscope the shower tracks in the nuclear emulsion plates and find the core structure. Energy measurement on every shower core can be made by counting number of shower tracks within a circle of various radii and at various thickness of lead in the chamber. The photometry measurement on darkness of a shower spot in X-ray films gives another way of energy determination.

Thus the emulsion chamber has several favourable points for observation of cosmic-ray events of high energy. First, it can provide a way of measuring accurately energy and location of gamma-rays and electrons, and, for application to cosmic-ray jets, it gives energy as well as emission angle of produced gamma-rays and neutral pions in a jet. The observation can be extended to include charged secondary particles in a jet, too, for cases of exposure with low background. Second, the stability and the economics allow one to construct the chamber with large area, say, a hundred m^2 or more, at a high mountain laboratory, and to expose it to cosmic-rays as long as one year or more. So, the statistics is greatly increased and the observation range is extended to much higher energy than before. Third, we can construct a complex of chambers for observation of arriving electrons and gamma-rays as well as hadrons.

As a typical example of the emulsion chamber experiment for jets, we will describe Brasil-Japan collaboration experiment with exposure at Mt. Chacaltaya Observatory, in Bolivia, of the height of 5200 m above sea level. The

structure of an emulsion chamber at Chacaltaya is composed of the four parts as shown in Fig. 6: 1) the upper detector, 2) the target layer, 3) the air gap and 4) the lower detector. We are concerned here with nuclear interactions produced in the target layer of petroleum pitch, whose thickness corresponds to $\sim 1/3$ mean free path for the nuclear interactions, or ~ 0.4 radiation length for the electro-magnetic processes. A high energy nuclear interaction from the target layer is called hereafter "C-jet", because the major composition of the target material is carbon.

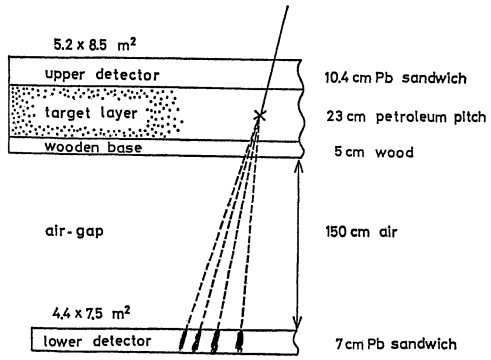

Fig. 6. Chacaltaya emulsion chamber of two-storey structure.
It is designed for observation of nuclear interactions at the target layer (C-jets).

Idea of this two-storey structure chamber comes from the following three considerations. First, the upper detector works as a shield against atmospheric gamma-rays and electrons coming into the target layer and the lower detector. Second, the target layer is made of low Z material, so that it is almost transparent to gamma-rays produced in C-jets. And, third, the travelling distance through the air gap gives enough separation among gamma-rays of a C-jet, so that, in the lower detector, the shower measurement is possible on the individuals without interference among the showers in a C-jet.

Now, the C-jet study can be performed as follows. One makes the X-ray film scanning for showers in the lower detector, and find events under a microscope in the nuclear emulsion plates. Then, one selects only those showers with their arrival direction passing through the upper detector, so that the selected ones are not side showers. Among them, the microscopic observation can pick up C-jets, since showers from a C-jet are with well-defined and well-distanced multiple cores, while the rest are either a single-core shower from a jet in the lower detector or a diffuse cascade-degraded shower from a jet in the upper detector.

The procedure of energy measurement of gamma-rays produced in a C-jet goes as follows. With the microscopic observation, the number of the shower tracks is counted in a circular area with a fixed radius, 50 μm in most cases, at successive nuclear emulsion plates in the detector. The transition curve of shower development is then constructed from the counting results at

various depths, and the energy estimation is obtained comparing the experimental one with the theoretical calculation by Nishimura.[7] The best fit is looked for allowing a shift Δt in the depth, so that it brings the two into the best agreement around the shower maximum. This shift Δt stands for depth of the first electron pair creation, and the procedure eliminates the largest part of fluctuation in the longitudinal developement of a cascade shower, i.e., the part depending on location of the first electron pair creation at the start of the cascade. Then, the statistical error in the shower size measurement will come mainly from the limited number of counted shower tracks, which gives a statistical error of the order of $\sim 10\%$ for a shower of a few TeV.

An experimental check and calibration in the absolute value can be made with the use of the kinematical relation on two gamma-rays from decay of a neutral pion. There holds the following relation giving the distance R_{12} between the two partner gamma-rays from a neutral pion decay as

$$R_{12} = h m_\pi c^2 / (E_1 E_2)^{1/2} , \tag{13}$$

where h is the distance to the point of decay vertex, and E_1 and E_2 are energies of the two gamma-rays.

Our observation on a C-jet gives the energy E_γ and the position $\boldsymbol{r}_\gamma$ at the plane of the detector for all the gamma-rays over the detection threshold. Being without information on energy of a jet-initiating incident hadron, E_0, we use the gamma-ray energy sum, $\sum E_\gamma$, as a measure for the interaction energy. The ratio, $k_\gamma = \sum E_\gamma / E_0$, is called the gamma-ray inelasticity. The emission angles of gamma-rays, θ_γ, are measured referring to the direction of energy center of the gamma-rays, given as,

$$\theta_\gamma = |\boldsymbol{r}_\gamma - \boldsymbol{R}| / h \tag{14}$$

with

$$\boldsymbol{R} = \sum E_\gamma \boldsymbol{r}_\gamma / \sum E_\gamma ,$$

where h is the distance from the observation plane to the vertex of the C-jet. The vertex is assumed at the middle of the target layer, so that the thickness gives at most deviation of $\sim 8\%$ in the value of h. For computation of the gamma-ray coordinate $\boldsymbol{r}_\gamma$ and the emission angle θ_γ, a correction is made for inclination of the arrival direction with the normal incidence to the detector plane.

It is to be noted that the above of reference axis for the direction variables of gamma-rays of a C-jet is different from the case of accelerator experiments, where all the variables are referred to the incident beam direction. Thus the angle θ_γ as well as $p_{t\gamma}$ here are defined with reference to the direction of C-jet energy center, so that they are expected to be slightly smaller in an average than those with the accelerator definition. Though this

choice of the reference is inevitable in the cosmic-ray experiment, it has such physical meaning that the reference is made to the moving direction of the leading fire-ball, instead of that of the incident hadron of a collision. A similar situation exists for the energy variables, too, because the cosmic-ray experiment does not give the incident energy E_0 itself. We shall use the fractional energy of gamma-rays, $f=E_\gamma/\sum E_\gamma$, in place of $x=E_\gamma/E_0$, the x-variable in the accelerator case.

§ 3. Energy and angular distribution of gamma-rays

3.1. *Test of scaling——Comparison with FNAL data*

"Scaling" is known as a remarkable characteristic of the hadron multiple production at the accelerator region below a few TeV. In order to see whether the scaling hypothesis is still valid in the cosmic-ray energy region of our concern, we constructed the inclusive distribution of energy and angle of gamma-rays out of C-jets of the highest energy group observed at Chacaltaya experiment. They are 80 C-jets satisfying the selection criterion of $\sum E_\gamma > 20$ TeV, far above the detection threshold in the X-ray film scanning for events. Observation of gamma-rays in each C-jet is under the detection restriction of $E_\gamma > 0.1 \sim 0.2$ TeV, and $\theta_\gamma < 10^{-3}$ radian, due to the limit of microscopic scanning in nuclear emulsion plates over the shower cores of C-jet.

For the comparison, a simulation calculation was made by Tabuki[8] on the basis of scaling extrapolation. He takes real events of 205 GeV proton collision observed by the hydrogen bubble chamber at FNAL, and converts the bubble chamber events into the cosmic-ray energy region applying Lorentz transformation. A value of the Lorentz factor, Γ, in the transformation is chosen randomly for each events, following the power law distribution with index -1.8, fitted to the hadron energy spectrum of cosmic-rays. Since the bubble chamber data do not have information on neutral pions, Tabuki assumes charge independence among the pions, converts the observed negative pions into the required neutral pions and makes them decay into two gamma-rays in an isotropic way in the π^0 rest system. Then we have the simulated raw cosmic-ray jet events under the scaling hypothesis.

Now the simulation of Chacaltaya C-jet experiment can be carried out in a straightforward way. One constructs the same geometry of apparatus in the computor, applies the same selection criteria for the C-jet events, imposes the same limit of detection to their gamma-rays and performs the same method of analysis on the artificial events. The result of this simulation calculation is shown together with experimental data from Chacaltaya emulsion chambers. Figure 7 gives the distribution of fractional energy, $f_\gamma=E_\gamma/\sum E_\gamma$, Fig. 8 of emission angle in log$\tan\theta$-scale, and Fig. 9 of transverse momentum $p_{t\gamma}$. The gamma-ray inelasticity k_γ is also computed, giving the average value as

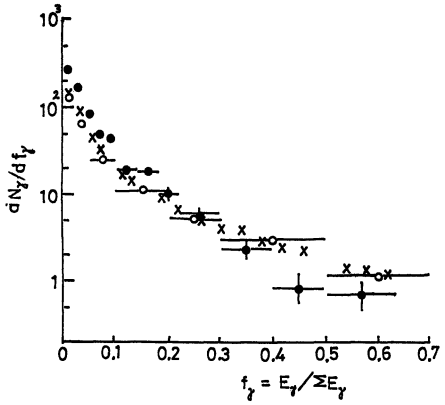

Fig. 7. Distribution of fractional energy $f_\gamma = E_\gamma / \Sigma E_\gamma$ of gamma-rays.
● 80 C-jets of Chacaltaya with $\Sigma E_\gamma > 20$ TeV.
○ scaling simulation from 205 GeV proton collisions in bubble chamber.
× scaling simulation from CERN ISR events.

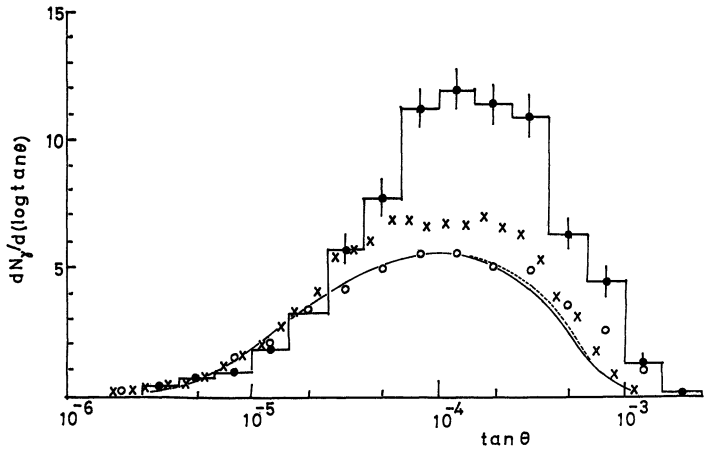

Fig. 8. Angular distribution of gamma-rays in logtanθ-scale.
● 80 C-jets of Chacaltaya with $\Sigma E_\gamma > 20$ TeV.
○ scaling simulation from 205 GeV proton collisions in bubble chamber.
× scaling simulation from CERN ISR events (—— ISR without successive interactions and - - - the same as above plus extended central plateau).

$\langle k_\gamma \rangle = 0.29$ for the present emulsion chamber experiment. We will use a value of $\langle k_\gamma \rangle = 0.3$ for the primary energy estimation hereafter, unless particularly stated.

3.2. *Test of scaling——Comparison with ISR data*

Arata[9] made another test of scaling on the basis of CERN ISR experiment of p-p collisions at $s^{1/2} = 53$ GeV. He starts from the experimental data of British-French-Scandinavian Collaboration with the split field facilities. In contrast to the case of bubble chamber experiments, there is a selec-

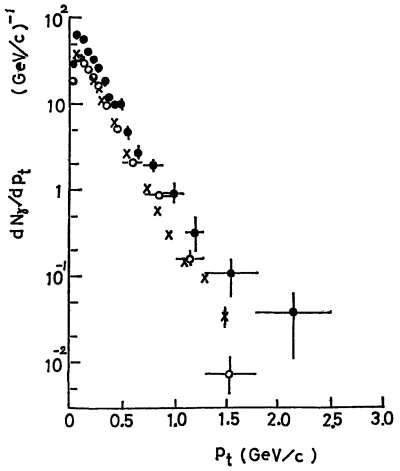

Fig. 9. p_t distribution of gamma-rays.
● 80 C-jets of Chacaltaya with ΣE_γ >20 TeV.
○ scaling simulation from 205 GeV proton collision in bubble chamber.
× scaling simulation from CERN ISR events.

tion bias of events due to the triggering condition and the detector does not cover the whole solid angle. Thus, Arata took the data of minimum-bias events and replaced their tracks missed in the observation by artificial tracks constructed by the Monte Carlo method. The Monte Carlo procedure for supplying the undetected tracks was constructed to give a fit with experimental results on the inclusive distributions of pions and the multiplicity distribution. The reconstructed minimum-bias events of ISR are composed of, on an average, observed tracks for 60% of the total and artificial Monte Carlo tracks for 40%. It should be remarked, therefore, that the events from ISR experiments include only a part of the correlation effects among the produced hadrons, but not the whole.

With the minimum-bias ISR events, Arata made the simulation calculation for Chacaltaya C-jet experiment in the same way as Tabuki did with FNAL bubble chamber events. The results are presented also in Figs. 7, 8 and 9 for the gamma-ray distributions on the fractional energy, on the emission angle in log$\tan\theta$-scale, and on transverse momentum. It is seen that the ISR simulation gives the results almost identical to those of the FNAL simulation, and both are significantly different from the cosmic-ray C-jet results.

Before concluding the discrepancy, we may add several remarks.

First is the effect of secondary hadron interactions in the emulsion chamber. Any of produced hadrons from an interaction in the target layer can produce, by chance, secondary interactions in the same layer, because the thickness of the target layer is not very small. Then, some of the observed C-jets can be a superposed result of successive events. Besides, those produced hadrons can make further secondary interactions in the lower detector, too, and the generated shower can be mistaken as an electron shower from a gamma-ray. Such effects of the secondary hadron interactions are included in the above simulation calculation, and the results show that the effects do not

influence the gross behaviour of produced gamma-rays in C-jets, as is demonstrated for the inclusive distribution in Fig. 8.

The second point is the contribution from the central plateau region of the collision system. It was argued by Ellsworth, Gaisser and Yodh[10] that boosting the accelerator events is not enough for the test of scaling extrapolation, because, as the collision energy goes higher, the current picture tells that the flat plateau in the rapidity scale extends and fills the central region. Arata estimated contribution to C-jets from the unsimulated part of the central plateau, and he found through the simulation calculation that gamma-rays from the unsimulated part are mostly with energy lower than the detection threshold and the contribution is of no importance to the conclusion. The results of his estimation is shown together in Fig. 8.

Thus, the conclusion is that the results of C-jets experiment are not on the scaling extrapolation of the accelerator results. The cosmic-ray C-jets have, on an average, larger multiplicity and larger p_t than those expected by scaling hypothesis.

A comment must be made on the simulation work of Ellsworth, Gaisser and Yodh,[11] who concluded that the cosmic-ray C-jet data can be explained by the scaling extrapolation of the accelerator results with inclusion of a large fraction of the hard scattering. Their agreement on p_t distribution with the C-jet data can be understood, because their model includes the hard scattering with large p_t for which they assume rapid increase with the collision energy. In fact, at the concerned cosmic-ray energy region, the contribution of high p_t pions from the hard scattering arrives at about 40% of the total produced pions in their assumed model. But, their results on the pion multiplicity, or more exactly, the gamma-ray rapidity density are hard to be understood. Their simulation calculation is with the x-distribution of pions from the accelerator experiments, so that the gamma-ray rapidity density of their model should coincide with the result of simulation by Tabuki, and by Arata. But their result is about twice larger than that of Tabuki and of Arata, giving an agreement with the experimental value from C-jet observation. Possible sources of the above discrepancy were looked for in every step, yet without success.

Finally it should be stressed that the "scaling" in multiple pion production, for a limited energy range of cosmic-ray energies ($\sum E_r = 0.3$–15 TeV),[15)~17)] was first found by cosmic-ray workers, about twenty years ago, earlier than Feynman proposal,[12] being known as the "similarity law".

3.3. *Comparison with SPS collider results*

The $\bar{p}$-p collider at CERN started its operation in 1981, and its preliminary results are now available on the particle multiple production at $s^{1/2} = 540$ GeV. The energy corresponds to $E_0 = 146$ TeV at the laboratory system. The results can be directly compared with the C-jet data with $\sum E_r > 20$ TeV,

because the average value, $\langle\sum E_\gamma\rangle\sim 40$ TeV, shows that the primary hadrons for those C-jets are with $\langle E_0\rangle\sim 120$ TeV.

Figure 10 is the comparison on the particle distribution on the rapidity scale compiled by Arata.[9] With the help of the simulation calculations given in 3. 2., he made all necessary corrections which originate from the cosmic-ray experimental conditions, and gave estimation on the unbiased distribution with incidence of a hadron with $E_0\sim 120$ TeV. It is shown in Fig. 10 together with the accelerator results[13] of SPS collider and of others with smaller energies. If we assume that pions are the major product of the collisions, we should expect that the particle number of gamma-rays and of charged hadrons will be in coincidence. While, the $\bar{p}$-p collider results show some difference between the two. The question whether the difference is real or not will be settled in the near future.

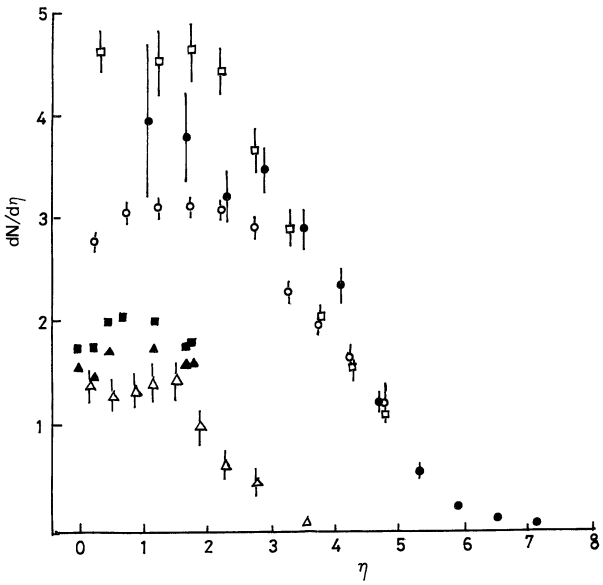

Fig. 10. Particle distribution on rapidity scale, η.
- ● gamma-rays from 80 C-jets of Chacaltaya with $\Sigma E_\gamma > 20$ TeV ($\sqrt{s}\sim 500$).
- □ gamma-rays from SPS $\bar{p}$-p collider, UA5 experiment.[13]
- ○ charged hadrons from SPS collider, UA5 experiment.[13]
- ■ gamma-rays from ISR ($\sqrt{s}=53$) experiment.
- ▲ gamma-rays from ISR ($\sqrt{s}=45$) experiment.
- △ gamma-rays from FNAL ($\sqrt{s}=19.7$) experiment.

Leaving such details for future, the results from C-jets and from $\bar{p}$-p collider are in good agreement. Thus, it is now clear that the rapidity density of produced hadrons is increasing with energy, and the argument raised by the simulation calculations by Ellsworth et al.[11] is settled. The increase of rapidity density amounts to about a factor 2, when the energy is increased to $E_0=120\sim 150$ TeV from $E_0=1\sim 2$ TeV. It means that the simple scaling rule with constant rapidity density does not work at the concerned energy region.

The comparison on p_t distribution can be made directly, because it is less affected by the observation conditions. From the SPS collider, the experiment UA-1[14] gives p_t distribution of charged hadrons and it is reproduced in Fig. 11 with corresponding data from ISR experiments. The result is to be

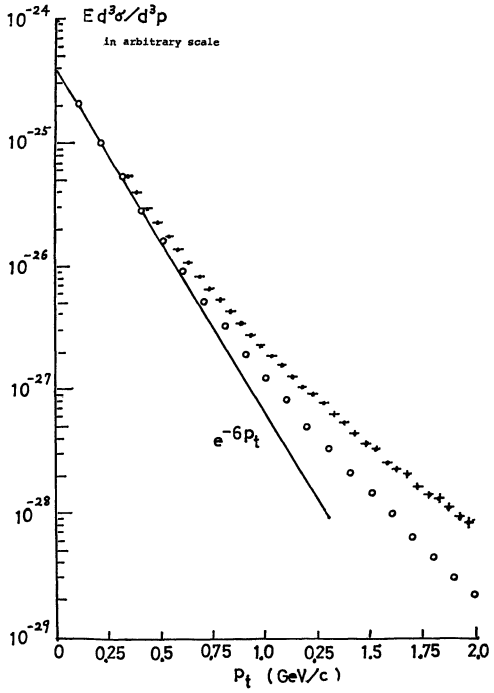

Fig. 11. p_t distribution of hadrons in SPS collider, UA1 experiment, together with result of ISR experiment.
+ $(h^+ + h^-)/2$ in SPS collider.
○ charged hadrons in ISR for $|y| \leq 1$.
Straight line expresses distribution of $\exp(-6p_t)$. Both results are normalized at $p_t = 0.3$ GeV/c.

compared with the cosmic-ray results on gamma-rays presented in Fig. 9 at 3. 2. It is seen in both figures that the distribution at $E_0 = 120 \sim 150$ TeV has larger tail of high p_t than that at lower energies of ISR and FNAL regions. The deviation begins appreciable beyond $p_t \sim 500$ MeV/c for gamma-rays or ~ 1 GeV/c for hadrons.

§ 4. Two types of jets

4. 1. *Early emulsion chamber results*

In the earlier observation at Mt. Chacaltaya before 1969, the chambers were of a small size and the observation was restricted in lower energy range, say, $\sum E_\tau = 3 \sim 15$ TeV for C-jets. What made us surprising through the earlier observation[15),16)] was a remarkable similarity of the phenomena of multiple production in different energy range. Combining the data from Chacaltaya with those from old experiments of balloon exposure,[17)] we had a rather wide observation range covering from $\sum E_\tau \sim 0.4$ TeV up to ~ 15 TeV. Within this range, p_t distribution was found unchanged, and the distribution of fractional energy, $f_\tau = E_\tau / \sum E_\tau$, too, was kept the same. Furthermore, both distributions, of p_t and of f_τ, were able to be described by a single and common functional form——an exponential function. Figure 12 presents a part of results of Chacaltaya experiment, exhibiting the constancy of fractional energy distribution

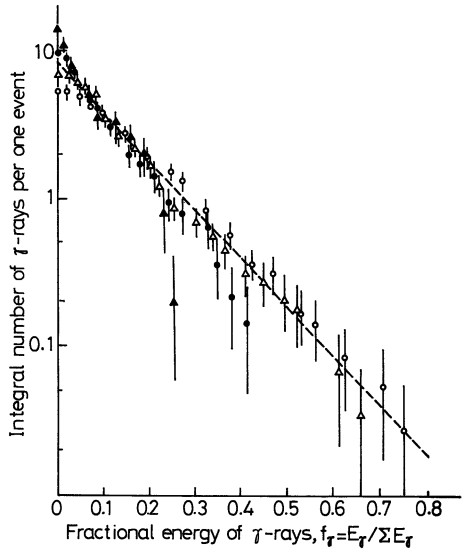

Fig. 12. Integral distribution of fractional energy for lower energy C-jets;
○: $3 < \Sigma E_\gamma < 5$ TeV,
△: $5 < \Sigma E_\gamma < 8$ TeV,
●: $8 < \Sigma E_\gamma < 15$ TeV,
▲: $\Sigma E_\gamma > 15$ TeV.
(The detection threshold for gamma-rays is ~0.2 TeV.)

in the observed jets.

The energy distribution of gamma-rays is practically equal to the momentum distribution of the longitudinal component along the jet axis. Thus the above similarity is exactly what should be expected from creation and decay of an isotropic fire-ball with constant rest energy and temperature, irrespectively of the magnitude of the interaction energy. One is, then, able to look for a coordinate system where both distributions of transverse and of longitudinal momentum become equal to each other. This is the system of a fire-ball at rest, and in the system, the gamma-rays are found to have the following momentum distribution:

$$\phi(p_\gamma^*)dp_\gamma^* = N_\gamma \exp(-p_\gamma^*/p_0)\frac{p_\gamma^* dp_\gamma^*}{p_0^2}\frac{d\Omega^*}{4\pi}. \qquad (15)$$

The asterisk expresses the quantity in the fire-ball system. The data at various $\sum E_\gamma$ interval can be fitted with a single set of parameter values, $N_\gamma = 8 \pm 1$ and $p_0 = 82 \pm 15$ MeV/c. Since the average momentum is given as $\langle p_\gamma^* \rangle = 2p_0$ in the distribution (15), one has estimation of gamma-ray part of rest energy of a fire-ball, $\mathfrak{M}_\gamma c^2$, as

$$\mathfrak{M}_\gamma c^2 = 2N_\gamma p_0 = 1.3 \pm 0.2 \text{ GeV}. \qquad (16)$$

We need a correction factor for the rest energy of a fire-ball itself, Mc^2, because $\mathfrak{M}_\gamma c^2$ covers only the fraction which goes into neutral pions. A simulation calculation shows that the correction factor under the charge independence is near a factor two, thus the rest energy is likely with a value between 2 and 3 GeV, which was already anticipated by the H-quantum model.

Soon after, we were informed that a remarkable characteristics——called as scaling—— was found in the hadron reactions by large proton accelerators. "Scaling" was understood as a possibility of describing multiple pion production by a single universal distribution function, irrespectively of the collision energy. Here they use the two variables, i.e., the transverse momentum p_t and the energy fraction, $x=E_\pi/E_0$. Leaving a difference in the reference of energy scale being either E_0 or $\sum E_\gamma$, which are connected through the gamma-ray inelasticity k_γ with each other, the accelerator results of "scaling" state the same facts as 20 year old "similarity law" in the distribution of fractional energy f_γ and of p_t. This agreement made us to think that the mechanism of multiple production of mesons is kept essentially unchanged throughout a wide range of energies starting from several ten GeV of accelerator region up to the cosmic-ray region of $\sum E_\gamma \sim 10$ TeV.

Among the community of high energy physics, there were arguments of Feynman[12] with an analogy to the bremsstrahlung in QED, and of Yang[18] with classical analogy of limiting fragmentation, as well as a number of works with application of Regge theory of meson reactions, called the theory of multi-peripheral collisions. All of these ideas predicted that the scaling rule would hold up to infinitely high energy region. Thus arose the name "asymptotia" for the region of extremely high energy, probably beyond $E_0 \sim 100$ GeV or so, where physics will be becoming monotonic and asymptotically constant. Under this ideology, the cosmic-ray work of extremely high energy would lose its raison d'être in the particle physics. Even the particle accelerator of very high energy could be doubted on its usefulness in comparison to its cost.

Already in 1968, we had an indication of the scaling break at higher energy region of $\sum E_\gamma \gtrsim 100$ TeV.[15),16] It was from the observation of atmospheric interactions (A-jets), where we found several events of large multiplicity and high p_t. If we interpret the events in terms of a fire-ball, we require the introduction of a heavier fire-ball than H-quantum. It was named as SH-quantum with estimated rest energy of $20 \sim 30$ GeV, average pion multiplicity of ~ 30 and $\langle p_{t\gamma} \rangle \simeq 250$ MeV/c.

4.2. *Phenomenological classification, Mirim- and Açu-jets*

The scaled-up experiment at Chacaltaya made us possible to observe a number of C-jet events with higher energy and some of them were found with large multiplicity and high p_t.

Leaving the interpretation for later studies, we classify the jets——the events of multiple pion production——into the two types, calling them "Mirim" and "Açu". "Mirim" and "Açu" are from Brazilian-Indian language, meaning small and big, respectively. Mirim-jets are those with common values of p_t and rapidity density, which are on the scaling extrapolation of low energy accelerator events. Açu-jets are with higher p_t and larger rapidity density than

the values from the scaling rule. With such phenomenological names of jets, we can express the scaling break, seen in the previous section, as appearance of Açu-jets at energy region as high as $E_0 \gtrsim 100$ TeV.

Let us now see how the phenomenological classification works on the observed events of C-jets. Figure 13 is the scatter plot of C-jets with $\sum E_\tau > 20$ TeV in the diagram of the average transverse momentum $\langle p_t \rangle$ and the average number of gamma-rays per unit rapidity interval, n_τ. In computing the above two quantities for each jets, the first gamma-ray is excluded in order to eliminate its large fluctuation effect. One sees that the experimental points scatter widely in the diagram, where one may recognize a cluster of events around $n_\tau \sim 7$ and $\langle p_t \rangle \sim 250$ MeV/c. But the scaling extrapolation of the accelerator events does not coincide with this cluster. It corresponds to the region around $n_\tau \sim 2$ and $\langle p_t \rangle \sim 150$ MeV/c, where one sees existence of another diffuse cluster of events. Figure 13 presents results of the simulation calculation of Tabuki[8] and Arata[9] on the same $\langle p_t \rangle$-n_τ diagram. Their calculations are with application of the scaling extrapolation to the events of FNAL and ISR. Comparing the figures, one finds that a diffuse cluster of events

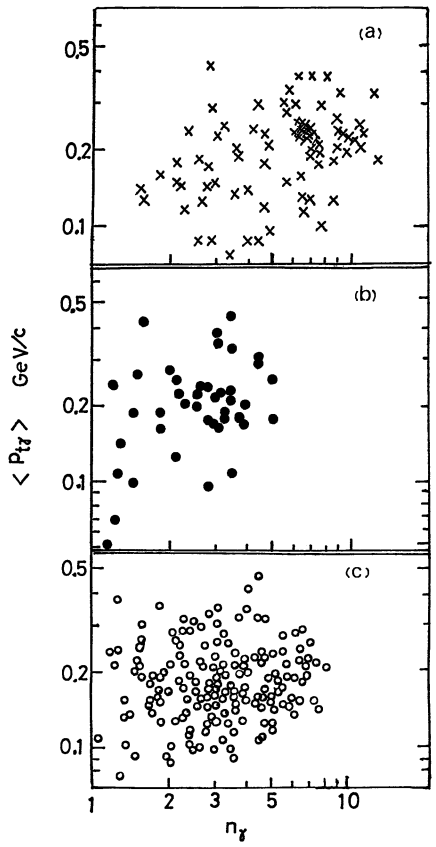

Fig. 13. Diagram of $\langle p_t \rangle$ and rapidity density n_τ of gamma-rays. Each point represents one event.
(a) 80 C-jets with $\sum E_\tau > 20$ TeV.
(b) scaling simulation events from 205 GeV p-p of FNAL.
(c) scaling simulation events from ISR min. bias events.

with $n_r = 2-4$ is in fact the one expected from the scaling extrapolation. They are of the type called as "Mirim". A collimated cluster of high multiplicity C-jets, $n_r = 6-8$, cannot be found in the scaling simulation. They are C-jets of a new type, which appear only in the cosmic-ray energy region and are responsible for the scaling break. They are the ones called "Açu".

It is interesting to look at the phenomenological classification from the composition of produced particles. The particle composition in multiple production events with $E_0 \lesssim$ several TeV has been known mainly of pions from old cosmic-ray observations and accelerator experiments. The problem gained a new attention of people after discovery of Niu and his colleagues in 1971[19] on heavy unstable particles of long life among the produced particles in a jet. The particle was named as X-particle, and later some of X-particles were found to be hadrons with charm. Since we do not know yet whether all X-particles are charmed ones or not, we will keep the name X-particle for the discussion.

There is a common impression among X-particle hunters that X-particles are always found in jets with large multiplicity. Among the reported six good examples of X-particles compiled by Niu,[20] there is no exception to the above empirical rule. The concerned events are with $E_0 \sim 10$ TeV, and Niu gave estimation of production rate as one X in $10 \sim 20$ jets. Sawayanagi[21] utilized the empirical rule, and searched X-particles in Chacaltaya C-jets of large multiplicity. He found four X-events among 24 such C-jets, giving the rate as one X in 6 high multiplicty jets with $\langle E_0 \rangle \sim 100$ TeV.

The above information indicates that Mirim-jets are with normal composition of pion majority and X-particles are associated with Açu-type jets. A sharp increase with energy of the production rate of charmed hadrons or X-particles can be one of the consequences of increasing fraction of Açu-jets at the nuclear collision. In this way, we may summarize our phenomenological classification as such that Mirim-jets are for the scaling while Açu-jets are for the scaling-break.

4.3. *Information from SPS collider*

We have so far not been informed on a conclusion from the $\bar{p}$-p experiments on our Mirim-Açu classification. So, the argument here is preliminary.

There is confirmation on the correlation between multiplicity and p_t. Figure 14(a) presents UA-1 results[22] on p_t distribution of hadrons for different multiplicity groups. For comparison, in Fig. 14(b), p_t distribution of gamma-rays is shown for Mirim and Açu C-jets of Chacaltaya experiment. One sees there is qualitative agreement between the two. The positive correlation between multiplicity and p_t is hard to be explained by general framework of a colliding system only, as is seen, for example, that the energy conservation may induce negative, but not positive, correlation. Its source must be looked for in the mechanism of multiple particle production itself.

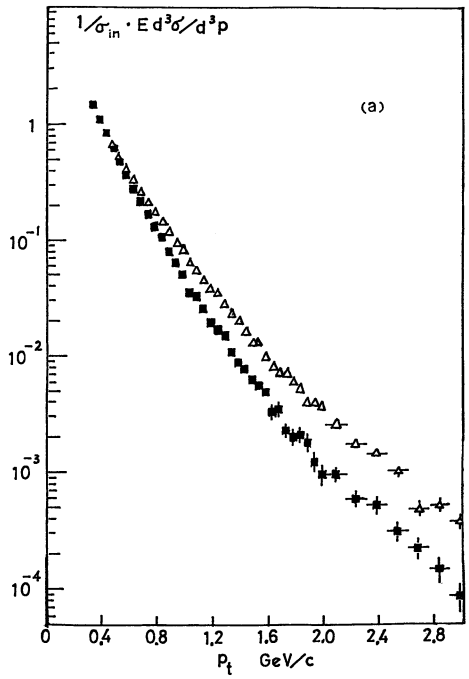

Fig. 14. (a) p_t distribution of hadrons for different multiplicity groups (UA1 experiment).
■: $5 \leq n \leq 25$, △: $40 \leq n \leq 100$.
Both distributions are normalized at $p_t = 0.3$ GeV/c.

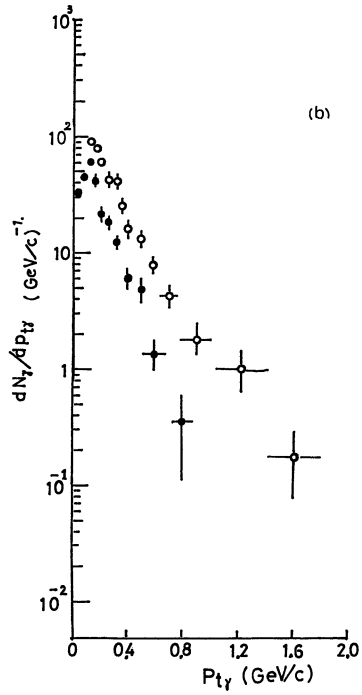

(b) p_t distribution of gamma-rays for Mirim- and Açu-jets.
●: 40 Mirim-jets,
○: 39 Açu-jets.

The product of multiplicity (or rapidity density) with $\langle p_t \rangle$ is the quantity representing amount of energy converted into heat (or heat density on rapidity scale) in a classical analogy. The measurement of UA-1 experiment[22] gives the information. Figure 15 presents their E_T distribution normalized per unit rapidity interval. In the same figure, the compiled result by Kumano[23] from Chacaltaya C-jet data is presented together. Since the C-jet measurement gives only the gamma-ray part, $E_T^{(\gamma)}$, the value is multiplied by 2.5 to convert into E_T itself. In their gross feature, E_T distribution from UA-1 and from C-jets are in agreement, while the one from NA-5[24] at CERN ($s^{1/2} = 24$ GeV) is much steeper.

From our phenomenological definition of the two types of jets, E_T distribution from NA-5 experiment of lower energy can be regarded as representing the distribution for the Mirim-type jets. The large deviation at higher E_T region, seen in the cosmic-ray and the $\bar{p}$-p collider experiment, is then interpreted as being caused by presence of Açu-jets. E_T distribution from the C-jet data is allowing such interpretation, since the events are seen to be composed

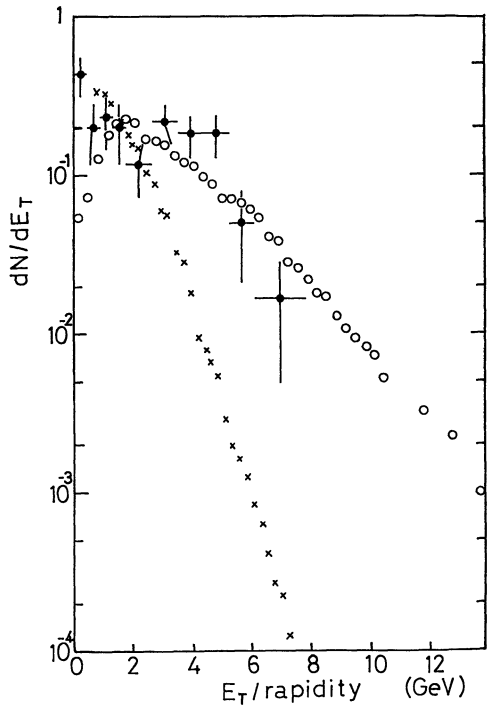

Fig. 15. Distribution of transversal energy flow per rapidity unit.
●: Chacaltaya C-jets with ΣE_T >20 TeV, $\sqrt{s}\sim$500 GeV.
○: SPS collider (UA1 experiment), $\sqrt{s}$=540 GeV.
×: NA5 experiment, $\sqrt{s}$=24GeV.

of two groups, one with $E_T \lesssim 2$ GeV of Mirim-type and another with $E_T \sim 5$ GeV of Açu-type.

While, E_T distribution from UA-1 experiment does not show such structure, being a smooth function without a bump. The double structure seen in C-jets may be a simple fluctuation. But at the same time, the triggering condition at UA-1 may distort the shape of distribution near the small E_T end. For the conclusion, we have to wait future studies with the $\bar{p}$-p collider.

Substantial changes in the characteristics of particle production are found by SPS collider experiment. They are mostly seen at high p_t region. It is informed that substantial yield of η-mesons is found at high p_t region by UA-5.[25] UA-5 experiment found sharp increase of p_t of strange particles, too.

Those suggest that the particle composition is changing at high p_t region, pions being not the major component anymore and heavier hadrons occupying a larger share. They will be, together with increasing yield of X-particles seen in cosmic-rays, a common syndrome due to presence of Açu-jets at energy region $E_0 \sim 100$ TeV.

§ 5. Quantum of fire-ball

5.1. *Mass spectrum of fire-balls*

For a cluster of gamma-rays from isotropic decay of a fire-ball, we are

able to estimate the rest energy either from their gamma-ray invariant mass, $\mathfrak{M}_r c^2$,

$$\mathfrak{M}_r c^2 = [(\sum E_i)^2 - (\sum p_i)^2]^{1/2} = (\sum E_i \cdot \sum E_i \theta_i^2)^{1/2} \tag{17}$$

or from the sum of gamma-ray transverse momenta, p_t,

$$\sum p_t = \sum E_i \theta_i \tag{18}$$

because there is a relation between the two, valid on an average, as,

$$\mathfrak{M}_r c = \frac{4}{\pi} \sum p_t \,. \tag{19}$$

Here, the summation covers over all the gamma-rays originating from the concerned fire-ball.

In the practical application, it is not always clear to see which gamma-ray belongs to the concerned fire-ball and to perform the summation without ambiguity. It is particularly so when the neighbouring fire-balls are close and the resulting clusters of gamma-rays are partially overlapping each other. Thus we have to find a method to define the cluster of gamma-rays corresponding to a fire-ball, for estimation of its rest energy. The method cannot be exact in every individual cases but must be correct on an average, and it must be objective and well-defined in the application. The constructed algorithm is described in an accompanying paper of Kumano.[23]

Figure 16(a) presents the histogram of gamma-ray invariant mass, $\mathfrak{M}_r$, obtained from 79 C-jets of Chacaltaya experiment with $\sum E_r > 20$ TeV. The C-jets are from the highest energy group because we tried to avoid the extrapolation method as much as possible. In most cases of lower energy C-jets, the observation range does not cover a whole cluster from the first fire-ball. The histogram of mass spectrum shows existence of two peaks, one with $\mathfrak{M}_r = 1-2$ GeV/c^2 and the other with $\mathfrak{M}_r = 4-7$ GeV/c^2. The first peak with $\langle \mathfrak{M}_r \rangle = 1.38 \pm 0.11$GeV/$c^2$ is from Mirim-jets, and the second peak with $\langle \mathfrak{M}_r \rangle = 5.40 \pm 0.25$ GeV/c^2 is from Açu-jets. The fire-ball corresponding to the first peak will be with the total rest energy $Mc^2 = 2-3$ GeV and can be identified to the H-quantum already discussed. The second peak shows existence of a heavier fire-ball, which we named as SH-quantum, i.e., abbreviation of super heavy quantum of a fire-ball. The rest energy of SH-quantum will be around 15$\sim$20 GeV, after multiplying with a factor three to $\langle \mathfrak{M}_r \rangle$, because the large multiplicity will diminish the effect of detection bias.

Accuracy of the rest energy estimation for a fire-ball is tested by the simulation calculation of Santos and Turtelli[26] for the H-quantum case, and Kamata and Yokoi for the SH-quantum case.[32] In their simulation to Chacaltaya C-jet

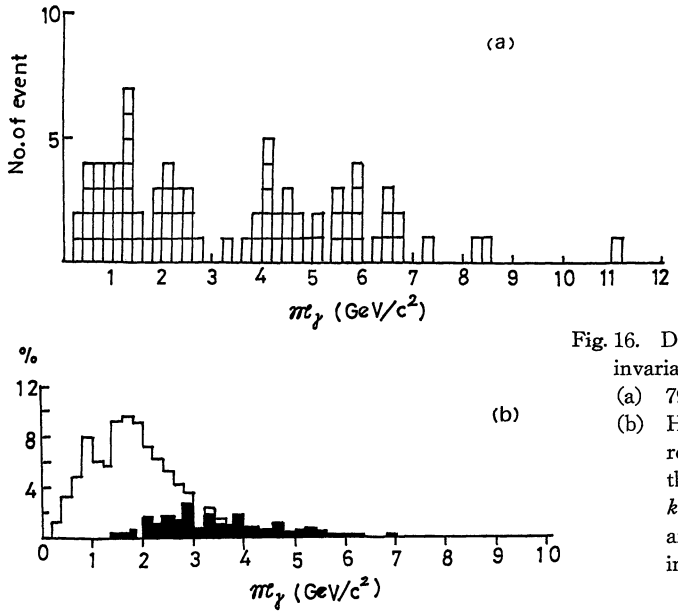

Fig. 16. Distribution of gamma-ray invariant mass $\mathfrak{M}_r$ of a fire-ball.
(a) 79 C-jets with $\Sigma E_r > 20$ TeV.
(b) Histogram shows simulation result under H-quantum hypothesis with $Mc^2 = 3$ GeV and $kT = 135$ MeV. Black parts are those with successive interactions.

experiment, they start with incoming cosmic-ray hadrons at the chamber with a power spectrum of energy with index -1.8, and let them make nuclear collisions in the target layer. At the interaction, they assume production of a fire-ball with rest energy Mc^2 decaying into pions with temperature kT. The inelasticity K of a collision is assumed to take random uniform values. Emission of pions from a fire-ball is computed with Monte Carlo method assuming isotropy and Planck distribution of momentum for pions. Then, neutral pions are made to decay into two gamma-rays and all the gamma-rays are followed down to the lower detector. For the outgoing nucleon and charged pions from a fire-ball, random sampling is made for further nuclear interactions in the rest of the target layer as well as in the lower detector. In this way, they constructed a large statistics of simulated C-jets with several parameter values of the fire-ball mass M and its decay temperature kT.

In Fig. 16(b), an example of the results of Santos and Turtelli[26] is shown on the histogram of gamma-ray invariant mass, $\mathfrak{M}_r$, where the parameter values are chosen as $M = 3\ \mathrm{GeV}/c^2$ and $kT = 135$ MeV, intending to represent the H-quantum case. The histogram in Fig. 16(b) is composed of the two parts; the blank part for pure cases without any secondary interactions and the shaded part for contaminated cases where successive nuclear interactions happen to occur. It is seen that the simulated mass spectrum yields a single peak at $\mathfrak{M}_r \sim 0.6\,M$ with a tail extending to high $\mathfrak{M}_r$ region. Through the comparison with the experimental histogram, one may conclude that the second peak in the experimental one cannot be simply due to successive interactions. Thus, it becomes reasonable to introduce a new heavy fire-ball, SH-quantum.

Comparison of the peak positions in the experimental and the calculated histogram tells us that the rest energy of the fire-ball responsible for the first peak in the experiment is $M=2-3\,\mathrm{GeV}/c^2$, and it is the H-quantum.

The case of SH-quantum was studied by Kamata and Yokoi, see the accompanying paper of theirs.[32]

5.2. *Overall view with H-quantum*

Let us try to construct a picture on the pion multiple production with the H-quantum hypothesis of a fire-ball. In a nuclear interaction of extremely high energies, a sequence of ν H-quanta will be produced along the incident direction of motion of colliding particles. Those H-quanta are assumed to move with Lorentz factors, $\Gamma_1, \Gamma_2, \cdots \Gamma_\nu$. Then the logtan$\theta$-plot of the jet will be a superposition of Gaussian distributions from isotropic emission with their respective centers at $1/\Gamma_1, 1/\Gamma_2, \cdots, 1/\Gamma_\nu$, respectively. The energy distribution will be approximated by superposition of exponential functions of a form, $\exp(-E/k\Gamma_i T)$ with $\mathrm{i}=1, 2, \cdots, \nu$, because emission of particles from an H-quantum will have a thermal distribution which can be approximated by an exponential function. The transverse momentum p_t of emitted partcles is composed of two parts, one from the particle emission out of H-quantum, and the other from the transverse motion of H-quantum itself.

It is immediately seen that the current gross picture of the pion multiple production in the accelerator region can be reproduced well, if the successive H-quanta are with constant relative motion between the consecutive ones, i.e.,

$$\Gamma_i/\Gamma_{i+1}=R \quad (i=1, 2, \cdots, \nu-1) \tag{20}$$

and the transverse motion of H-quanta does not give a significant contribution. For cases with R being not very large, say less than 10, the neighbouring H-quanta will produce overlapping pion clusters, so that the superposed distribution of pions will appear just continuous and smooth. The superposed logtanθ-plot will have a flat distribution——plateau——over the central part, and the energy distribution can be approximated as dE/E except for the highest and the lowest energy ends,

Now we will look into the experimental data of C-jets of Mirim-type from such point of view. Figure 17 presents the scatter diagram on θ_γ and p_t of all gamma-rays of Mirim C-jets of Chacaltaya experiment, 40 events, selected with the criterion $\sum E_\gamma > 20$ TeV. The angles are represented on the scale of $\log(\theta_\gamma \sum E_\gamma)$ to normalize differences of the interaction energy $\sum E_\gamma$ among the events. In terms of the fire-ball language, we may approximate $\sum E_\gamma$ with $\Gamma_1 \mathfrak{M}_\gamma c^2$, Γ_1 being the Lorentz factor of the first fire-ball, so that we have,

$$\theta_\gamma \sum E_\gamma = \mathfrak{M}_\gamma c^2 \tan \theta^*/2\,, \tag{21}$$

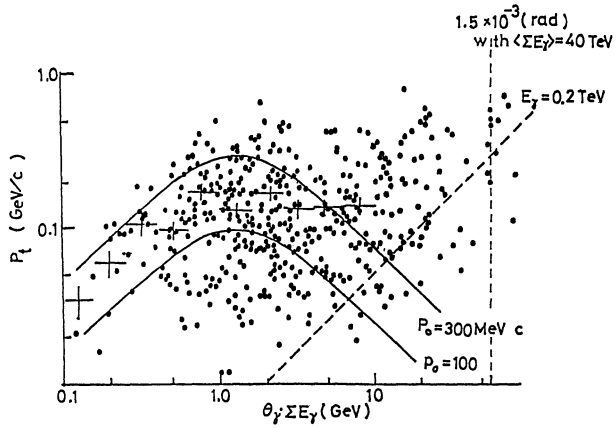

Fig. 17. Diagram of gamma-rays on p_t and energy-normalized emission angle $\theta_\gamma \Sigma E_\gamma$. Data are from 40 C-jets of Mirim-type with $\Sigma E_\gamma > 20$ TeV. Broken lines show the limit of detection. Cross represents average p_t over respective bin in the emission angle. Full line gives expected variation of p_t vs θ from the isotropic fire-ball assumption.

where θ^* is the emission angle in the first fire-ball rest frame. Therefore, the position of the first H-quantum center is at the point of $\mathfrak{M}_\gamma c^2$ in this scale. Since one has $\langle \mathfrak{M}_\gamma c^2 \rangle = 1.38 \pm 0.11$ GeV from the previous estimation of gamma-ray invariant mass, one expects clustering of points in the diagram at around $\sim$1.4 GeV, showing gamma-rays emitted from the first H-quantum. In the plot of Fig. 17, one recognizes a tendency of such expected clustering. At the same time, one sees that the continuous and uniform distribution of gamma-ray points extends over a region of larger angles in the diagram up to a point where the detection threshold starts to operate for missing particles. It indicates contribution from the next gamma-ray cluster of the second H-quantum with partial overlapping to the first one.

Figure 18 is the spectrum of fractional energy of gamma-rays, f_γ, for the Mirim-jets, together with that of Açu-jets for comparison. Following the previous argument, we expect that the f_γ-spectrum can be expressed as,

$$\phi(f_\gamma) df_\gamma = N_\gamma^2 \exp(-N_\gamma f_\gamma) df_\gamma , \qquad (22)$$

where N_γ expresses number of gamma-rays from an H-quantum. This is only a part from the first H-quantum, and, in Fig. 18, the expected distribution is shown for a case with $N_\gamma = 6$. It is seen that the experimental one is just as expected in the region of large $f_\gamma \gtrsim 0.1$, while, in smaller f_γ region, one recognizes a rise of the distribution coming from the consecutive H-quanta.

It is possible to make a detailed observation on the first H-quantum, because both the detection threshold and the overlapping from the neighbouring H-quantum least affects the observation. Under the isotropic assumption,

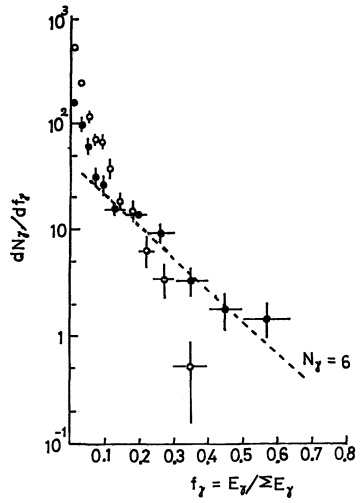

Fig. 18. Spectrum of fractional energy, f_γ, of gamma-rays.
●: 40 C-jets of Mirim-type with $\Sigma E_\gamma > 20$ TeV.
○: 39 C-jets of Açu-type with $\Sigma E_\gamma > 20$ TeV.
Dotted line represents the case for $N_\gamma = 6$.

one expects the variation of p_t with the emission angle θ^* from the relation

$$\langle p_t \rangle = p_0 \sin \theta^* , \tag{23}$$

where the average is taken over a certain interval of the emission angle. The constant p_0 is the average momentum in the coordinate system of an H-quantum at rest. The curves in Fig. 17 show the above relation with several values of p_0. One sees that the experimental value of $\langle p_t \rangle$ shows such variation with emission angle θ^*, at least in the forward half of the first H-quantum. Its backward half is seen obscured by the overlapping with the second H-quantum. Such variation of $\langle p_t \rangle$ gives us a conclusion that the momentum of gamma-rays in the H-quantum system, p_0, is a quantity more basic than the transverse momentum p_t.

5.3. *H-quantum in accelerator region*

It has already been shown that the H-quantum model explains gross behaviour of multiple production of mesons in the accelerator region, because the model provides constancy of p_t, scaling of longitudiñal momentum distribution, plateau in the logtanθ-plot of angular distribution, and logarithmic increase of the multiplicity. In short, the H-quantum model is one of the so-called "ln-s physics". What is particular for the H-quantum model will be discontinuity due to presence of the energy quantum in the phenomena, in contrast to other models of ln-s physics. We tried to observe such discontinuity in the cosmic-ray phenomena but so far not yet very successful. The accelerator experiments can have a chance to see the discontinuity, because of their better accuracy compared to the cosmic-ray cases.

One example of expected discontinuity will be the threshold behaviour at production of an H-quantum. A preliminary study was made by Tanaka,

Nanjo and others[27] with the hydrogen bubble chamber film analysis on interactions of 10 GeV/c negative pions of CERN. Assuming the final state being of the three particles, i.e., a leading pi-meson, a recoil proton and a created fire-ball, the kinematics allows that the rest energy of a fire-ball can be 3.36 GeV at the maximum. Thus the studied collision will be just above the threshold of a single H-quantum production.

Out of 675 events of nuclear interaction observed, they made detailed study on events with large prong number, i.e., $n=6$, 8 and 10, which are 90 events occupying about 13% of all. The studies on large multiplicity cases were found to be well consistent with a single H-quantum production with rest energy 2.4 ± 0.4 GeV of the same decay mode as in the case of cosmic-ray studies. Among the small multiplicity events, i.e., $n=2$ and 4, some can be also due to production of an H-quantum decaying with a number of missing neutral particles, but the majority cannot. Thus, they came to the view that at this energy just above the threshold, there are two channels in the meson production. One is the production and decay of a single H-quantum, and the other is with less multiplicity, and can be regarded as continuation of plural meson production of lower energy region.

One can imagine that a similar situation will be found near every threshold of plural production of H-quanta. For example, around the threshold for ν H-quanta production, one will see existence of competing channels, such as ν H-quanta production and $(\nu-1)$ H-quanta production accompanied with production of a hadron resonance, and so on. Those situation will mask the discontinuity of the phenomena with the quantum emission and smooth out the variation in multiple meson production. Thus the experimental detection of the discontinuity will be not easy task even with the accelerators.

§ 6. Heavier fire-balls

6.1. *Cosmic-ray families with emulsion chamber*

An emulsion chamber detects a bundle of electrons, gamma-rays and hadrons which we call "the cosmic-ray family". The bundle is a result of atmospheric nuclear and electromagnetic cascades originating from arrival of a single primary cosmic-ray particle at the top of atmosphere. The name "family" expresses such genetic relation among particles in a bundle. Observation of a family with an emulsion chamber is a powerful tool to investigate the nuclear interactions of energy range $E_0=10^{14}$—10^{16} eV and beyond.

Figure 19 demonstrates how the emulsion chamber detects such family of cosmic-rays. Gamma-rays and electrons, on arrival at the chamber, generate electron showers as soon as they enter into the lead-sandwich. Thus the showers starting near the top of the emulsion chamber (upper part of the upper chamber in the figure) are likely to be from atmospheric electrons or

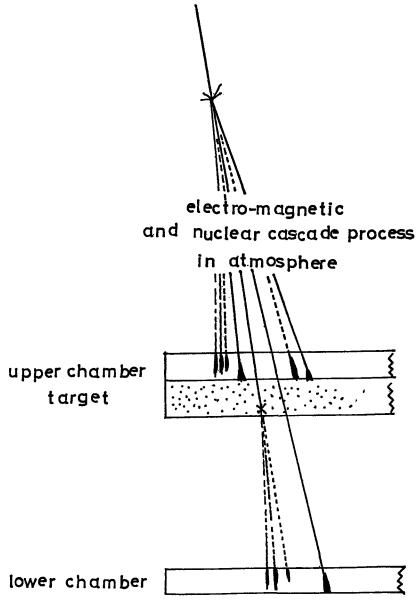

Fig. 19. Illustration of a family, after generated from A-jets, arriving at the emulsion chamber. —— for hadrons and ---- for electrons and gamma-rays.

gamma-rays—we abbreviate them simply (e, γ), since the observation with an emulsion chamber has no way to distinguish between electrons and gamma-rays.

Hadrons are detected through an electron shower generated by their local nuclear interactions in the chamber itself. Because of large penetrating power of hadrons than of (e, γ), the shower from a local nuclear interaction can happen at any place in the chamber. We call them Pb-jet and C-jet, differentiating them whether the nuclear interaction happens to be in the lead-sandwich or in the target layer. Pb-jets are divided into two, Pb-jet-upper and -lower, distinguishing their location being whether in the upper chamber or in the lower one. When a Pb-jet-upper happens to occur near the top surface of the chamber, its shower can be mixed up with a shower from (e, γ).

A family has full of varieties in its appearance, because it is at the very initial stage of the atmospheric cascades. A large part of the fluctuation in the appearance of a family is coming from variation in position of its parent atmospheric nuclear interactions. When it is high in the atmosphere, the produced gamma-rays will suffer the electro-magnetic cascade process of multiplication and degradation in their atmospheric passage. In such cases, the appearance of a family will be dominated by the characteristic features of electromagnetic cascades. On the other hand, when the parent interaction is located near the chamber, say within several hundred meters in distance, the electro-magnetic cascade process in the atmosphere will not make any significant contributions. We will call such cases as "a clean family". The observation of a clean family gives us directly the energy and angular distribution of gamma-rays produced in the parent nuclear interaction, which we

will call A-jet hereafter. There are, of course, mixed cases where a part is clean and the rest of the family is with electro-magnetic cascades. In fact, the majority of observed families are of such complex character coming from successive nuclear interactions in the atmosphere.

The study on A-jets through observation of a clean family has been a heuristic method in investigation of unknown world of extremely high energy nuclear interactions. For example, it was as early as in 1968 that we noticed existence of A-jets with significantly larger multiplicity and p_t. Only after several years, such Açu-type jets were confirmed by the C-jet experiment. This is because that the A-jet study through observation on clean families is more efficient way than C-jet study, in the sense that the frequency of events can be increased and the observation range can be extended to much higher energy.

6.2. *Jet of very large multiplicity——Guaçu-jet*

Direct observation of interactions with very large multiplicity, if it exists, has been one of the main issues of the emulsion study on cosmic-rays. In particular, the A-jet study with clean family observation will be a most promising way to look for such type of nuclear interactions.

There was a report of Perkins and Fowler[28] on one of such examples of very large multiplicity events, named "Texas Lone Star". It is a bundle of more than two hundred gamma-rays with the total energy $\sum E_r \sim 140$ TeV, produced by a nuclear interaction just outside their emulsion stack of balloon exposure. The log$\tan\theta$-plot of the event is presented in Fig. 20 showing enormous multiplicity. However, a possibility remains that the incident particle might not be a proton but an alpha-particle, which occupies non-negligible part of the hadron flux at the high atmosphere.

From observation with Chacaltaya emulsion chamber, we will present a few examples which directly exhibit the nuclear interaction of abnormally large multiplicity. Two are clean A-jets occurring near the chamber, and the last is a C-jet. Thus we know existence of the nuclear interactions with very large multiplicity, far exceeding the case of Açu-jet. We will call it as Guaçu-jet, meaning very large in old Brazilian-Indian language.

A family No. 112-S in Chamber No. 17 has almost no trace of atmospheric cascades as far as we look at the event in X-ray films. The detailed study of the event was carried out by Semba,[29] outline of which will be presented here. He made detailed microscopic study in the nuclear emulsion plates over a circular area of radius 2 mm around every shower detected by the X-ray film spot scanning. It is found that $\sim 60\%$ of the showers are really with a single core and the rest are with narrowly collimated multiple cores, telling that the coming-in bundle of particles are mostly gamma-rays direct from the nuclear interaction. A quantitative study was made with a simulation calculation on atmospheric electron cascade processes starting from A-jet of

various assumed production heights. The comparison gives a conclusion that the height of A-jet is 250 ± 80 m. Contribution of electrons and gamma-rays originating from the ancestral interactions at upper atmosphere cannot be completely excluded but are not significant.

Recently, we found a clean family of similar type in chamber No. 19, called event No. 191-S with $\sum E_\gamma = 256$ TeV. Semba[30] applied the same method of analysis to the new event and obtained the estimation of the height of nuclear interaction as 320 ± 80 m.

There is a C-jet with very large multiplicity and large p_t. The event is named as No. 153-I in chamber No. 17, and it has 41 shower cores with total energy $\sum E_\gamma = 42$ TeV, spreading over a circular area of radius ~ 5 mm in the emulsion plate of the lower chamber. The analysis was carried out by Arata.[31] Since this C-jet is a member of large family with the total visible energy $\sum E_\gamma \sim 293$ TeV spreading over an area of radius ~ 3 cm, a possibility was examined whether the event is just a single C-jet or is composed of a narrowly collimated group of two or more C-jets. The measurement on direction of shower cores in the C-jet shows that they are convergent into one point in the target layer and the event is regarded as a single C-jet.

In Fig. 20, the logtanθ-plot for gamma-rays is shown for the above two A-jets, No. 112-S in chamber No. 17, and No. 191-S in chamber No. 19, and a C-jet No. 153-I in chamber No. 17, together with that of Texas Lone Star. It is seen that the density of gamma-rays in the rapidity scale is much higher in all the cases than the case of Açu-jets. The C-jet, No. 153-I, was unfortunately with such low energy that the detection threshold gives rather severe

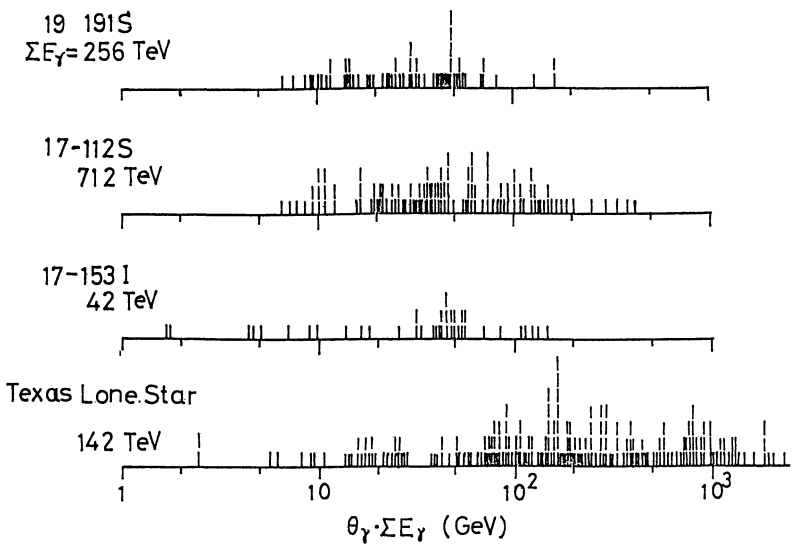

Fig. 20. logtanθ-plot of large multiplicity events of Guaçu-type.

restriction on the observation range so that we can see only a part of the whole event.

6.3. *SH- and UH-quantum*

We have seen the existence of two new types of pion multiple production, characterized by their large p_t and large multiplicity, and they are called Açu-jet and Guaçu-jet, meaning "large" and "very large" jet in Brazilian-Indian language. The H-quantum is now not the only intermediate product of extremely high energy nuclear collisions. Under the fire-ball hypothesis, we have to introduce new kinds of a fire-ball with large rest energy and high decay temperature. In this way, we proposed SH-quantum (super heavy quantum) for the one responsible to Açu-jet, and UH-quantum (ultra heavy quantum) to Guaçu-jets.

An analysis was made on Açu-jets and Guaçu-jets under the hypothesis of SH-quantum and UH-quantum, in a parallel way what we did for Mirim-jets with H-quantum assumption. The result shows some indication that a straightforward analogy to the H-quantum case does not give a resonable agreement with experimental data, even if the parameters, the rest energy $\mathfrak{M}_r$ and the decay temperature kT, are changed in wide interval. For example, the

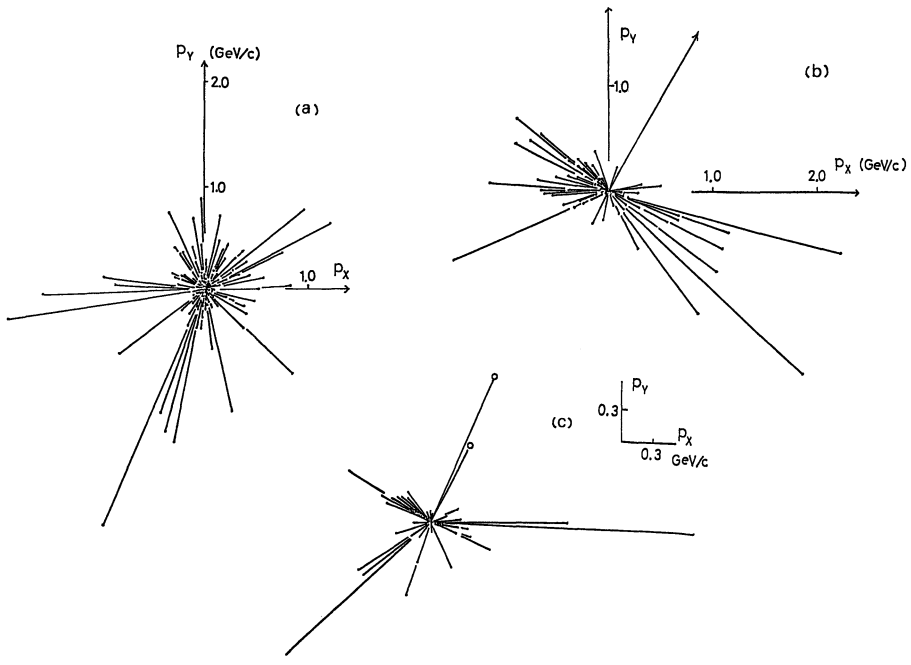

Fig. 21. Gamma-rays in p_t-plane. Three Guaçu-jets are presented.
(a) A-jet #112S in chamber No. 17.
(b) A-jet #119S in chamber No. 19.
(c) C-jet #153I in chamber No. 17.

distribution of p_t and of fractional energy f_r for Açu- and Guaçu-jets are not exactly of an exponential form but have a larger tail. A consistent agreement can be obtained with the assumption of successive decay of SH- and UH-quanta, not directly going into pi-mesons but through H-quanta. The detailed study was made by Kamata and Yokoi[32] and their results are presented in an accompanying paper. This idea of successive decay through H-quanta is more attractive than that of simple direct decay, because the H-quantum is assumed as the basic unit of multiple production of mesons.

Figures 21 (a)$\sim$(c) present the three events of Guaçu-jet in the p_t plane of the gamma-ray momenta, where individual observed gamma-rays are represented by a vector. The distribution of gamma-ray vectors appears somewhat different from what we will expect from the direct isotropic decay into pi-mesons. We may recognize a clustering of vectors, which can be called multi-jet structure. Such multi-jet structure can be expected from the successive decay, where intermediate H-quanta are represented by respective jets. The successive decay through H-quanta enhances fluctuations in the pion distributions in the final states, so that the previous way of estimating physical constants for the fire-balls on the basis of isotropic decay may not give so accurate results as the case for the direct decay.

§ 7. Conclusions

Systematic observation is made on gamma-rays produced from the nuclear interactions at the target layer (C-jets). The study leads us to identify the following three phenomenological types among the events of pion multiple production. "Mirim"-jets are those on the simple scaling extrapolation from the accelerator energy region around 1 TeV. "Açu"-jets are the cause of scaling-break, and their frequency increases with energy and arrives at about 50% of the events with $E_0\sim$100 TeV. "Guaçu"-jets are found, in most of cases, in the atmospheric nuclear interactions (A-jets) with higher energy,

Three phenomenological types of pion multiple production.

name of type (meaning)	Mirim (small)	Açu (large)	Guaçu (very large)
characteristics of produced gamma-rays			
a) rapidity density	2$\sim$3	6$\sim$8	20$\sim$30
b) $\langle p_t \rangle$ in MeV/c	140	220	400$\sim$500
c) p_t flow/rapidity in GeV/c	0.2$\sim$0.5	1.0$\sim$2.0	10$\sim$20
composition	mainly pions	mostly pions with non-negligible yield of heavier particles	
observed number of C-jets (ΣE_r>20 TeV)	40	39	1

$E_0 \sim 1{,}000$ TeV.

Analysis is made with the fire-ball model, and the three kinds of a fire-ball quantum are postulated. They correspond to the above three types of jets. The table gives estimated values for the physical parameters of the proposed quanta.

Three kinds of fire-ball quantum.

name of fire-ball quantum	H-quantum (heavy quantum)	SH-quantum (super heavy quantum)	UH-quantum (ultra heavy quantum)
corresponding type of jets	Mirim	Açu	Guaçu
rest energy in GeV			
a) gamma-ray part	1.3	5∼10	30∼ 80
b) total	2∼3	15∼30	100∼300
proposed decay mode	into pions	first into H-quanta, and then pions (non-negligible presence of heavier hadrons)	

Acknowledgements

The collaboration experiment is financially supported in part by Conselho Nacional para o Desemvolvimento Científico e Tecnológico, Fundação de Amparo à Pesquisa do Estado de São Paulo, in Brasil, and Institute for Cosmic-Ray Research, University of Tokyo and Grant-in-Aid from the Ministry of Education, in Japan.

References

1) G. Wataghin, *Proc. Symp. Cosmic-Rays* (Academia Brasileira de Ciencia), (1941).
2) E. Fermi, Prog. Theor. Phys. **5** (1950), 570.
3) K. Niu, Nuovo Cim. **10** (1958), 994.
P. Ciok, T. Coghen, J. Gierula, R. Holinski, A. Jurak, M. Miesowitz, T. Saniewska and O. Stanisz, Nuovo Cim. **8** (1958), 166; **10** (1958), 741.
G. Cocconi, Phys. Rev. **111** (1958), 1699.
4) S. Hasegawa, Prog. Theor. Phys. **26** (1961), 151; **29** (1963), 128.
5) S. Hasegawa and K. Yokoi, *Proc. Int. Conf High Energy Phys.* (CERN), (1962).
6) G. Fujioka, Y. Maeda, O. Minakawa, M. Miyagaki, I. Mito, K. Kobayakawa, H. Shimoida, N. Nakatani, O. Kusumoto, K. Niu and K. Nishikawa, Nuovo Cim. Suppl. **1** (1963), 1143.
7) J. Nishimura, Handbuch der Physik, Vol. XLVI (1967), 1; Prog. Theor. Phys. Suppl. No. 32 (1964), 72.
8) T. Tabuki, Prog. Theor. Phys. Suppl. No. 76 (1983), 40.
9) N. Arata, Nucl. Phys. **B211** (1983), 189.
10) R. W. Ellsworth, G. B. Yodh and T. K. Gaisser, AIP Conf. Proc. No. 49 (1979), 111.
11) R. W. Ellsworth, T. K. Gaisser and G. B. Yodh, Phys. Rev. **D23** (1981), 764.
12) R. Feynman, Phys. Rev. Lett. **23** (1969), 1415.
13) UA5 Collaboration (Bonn-Brussel-Cambridge-CERN-Stockholm), Production of Photons and Search for Centauro Events at the SPS Collider (CERN-EP/82-60).
14) UA1 Collaboration (Aachen-Annecy-Birmingham-CERN-Helsinki-Queen Mary College-

Paris-Riverside-Roma-Rutherford-Appelton-Saclay-Wien), Report for Quark-Lepton Conference, Stockholm, June 1982.
15) M. Akashi, Z. Watanabe, K. Nishikawa, Y. Oyama, M. Hazama, T. Ogata, T. Tsuneoka, T. Shirai, A. Nishio, I. Mito, K. Niu, I. Ohta, T. Taira, J. Nishimura, N. Ogita, Y. Fujimoto, S. Hasegawa. A. Osawa, T. Shibata Y. Maeda and C. M. G. Lattes, N. M. Amato, D. V. Fereira, C. Aguirre, M. Schonberg, M. S. M. Mantovani, Can. J. Phys. **46** (1968), 660.
16) C. M. G. Lattes, M. S. M. Mantovani, C. Santos, E. H. Shibuya, A. Turtelli Jr., N. M. Amato, A. M. F. Endler, M. A. B. Bravo, C. Aguirre and M. Akashi, Z. Watanabe, I. Mito, K. Niu, I. Ohta, A. Osawa, T. Taira, J. Nishimura, Y. Fujimoto, S. Hasegawa, K. Kasahara, E. Konishi, T. Shibata, N. Tateyama, N. Ogita, Y. Maeda, K. Yokoi, T. Tsuneoka, A. Nishio, T. Ogata, M. Hazama, K. Nishikawa, Y. Oyama, S. Dake. Prog. Theor. Phys. Suppl. No. 47 (1971), 1.
17) O. Minakawa, Y. Nishimura, M. Tsuzuki, H. Yamanouchi, H. Aizu, H. Hasegawa, K. Ishii, S. Tokunaga, Y. Fujimoto, S. Hasegawa, J. Nishimura, K. Niu, K. Nishikawa, K. Imaeda and M. Kazuno, Nuovo Cim. Suppl. **11** (1959), 125.
18) J. Benecke, T. T. Chou, C. N. Yang and E. Yen, Phys. Rev. **188** (1969), 2159.
19) K. Niu, E. Mikumo and Y. Maeda, Prog. Theor. Phys. **46** (1971), 1644.
20) K. Niu, AIP Conf. Proc. No. 47 (1979), 181.
21) K. Sawayanagi, Phys. Rev. **D20** (1979). 1037.
22) UAI Collaboration, see Ref. 14).
23) H. Kumano, Prog. Theor. Phys. Suppl. No. 76 (1983), 51.
24) K. P. Pretzl, AIP Conf. Proceedings, No. 85 (1982), 585.
25) UA5 Collaboration (Bonn-Brussels-Cambridge-CERN-Stockholm), Strange Particle production at the CERN SPS Collider (CERN-EP/82-61, 26 May 1982).
26) M. C. B. Santos and A. Turtelli Jr., Conf. Papers, 16th Int. Cosmic-Ray Conf. Vol. 6 (1979), 274.
27) S. Hasegawa, H. Nanjo, T. Ogata, M. Sakata, K. Tanaka and N. Yajima, Prog. Theor. Phys. Suppl. No. 47 (1971), 126.
28) D. H. Perkins and P. H. Fowler, Proc. Roy. Soc. **A278** (1964), 401.
29) H. Semba, Nuovo Cim. **49A** (1979), 247.
30) H. Semba, Conf. Papers, 17th Int. Cosmic-Ray Conf. Vol. 11 (1981), 95.
31) N. Arata, Nuovo Cim. **43A** (1978), 455.
32) S. Kamata and K. Yokoi, Prog. Theor. Phys. Suppl. No. 76 (1983), 83.